Received: 4 June 2020 | Revised: 30 September 2020 | Accepted: 2 October 2020

DOI: 10.1002/pro.3963

THE PROTEIN SOCIETY WILEY

ARTICLE

Kinetic characterization and structure analysis of an altered polyol dehydrogenase with D-lactate dehydrogenase activity

Diane Chauliac[1,4] | **Qingzhao Wang**[1,5] | **Franz J. St. John**[2] | **Grace Jones**[3] | **Jason C. Hurlbert**[3] | **Lonnie O. Ingram**[1] | **Keelnatham T. Shanmugam**[1]

[1]Department of Microbiology and Cell Science, University of Florida, Gainesville, Florida

[2]Forest Products Laboratory, USDA Forest Service, Madison, Wisconsin

[3]Department of Chemistry, Physics and Geology, Winthrop University, Rock Hill, South Carolina

[4]Galactic, Brussels, Belgium

[5]BP Bioscience Center, San Diego, California

Correspondence
Franz J. St. John, USDA Forest Service, Forest Products Laboratory, One Gifford Pinchot Drive, Madison, WI 53726, USA.
Email: fjstjohn@gmail.com; franz.j.st.john@usda.gov

Funding information
National Center for Research Resources, Grant/Award Number: 5 P20 RR016461; U.S. Department of Agriculture, Grant/Award Number: 2011-10006-30358; U.S. Department of Energy, Grant/Award Numbers: DE-PI0000031, W-31-109-Eng-38

Abstract

During adaptive metabolic evolution a native glycerol dehydrogenase (GDH) acquired a D-lactate dehydrogenase (LDH) activity. Two active-site amino acid changes were detected in the altered protein. Biochemical studies along with comparative structure analysis using an X-ray crystallographic structure model of the protein with the two different amino acids allowed prediction of pyruvate binding into the active site. We propose that the F245S alteration increased the capacity of the glycerol binding site and facilitated hydrogen bonding between the S245 γ-O and the C1 carboxylate of pyruvate. To our knowledge, this is the first GDH to gain LDH activity due to an active site amino acid change, a desired result of in vivo enzyme evolution.

KEYWORDS

Bacillus coagulans, directed evolution, D-lactic acid, glycerol dehydrogenase, lactate dehydrogenase

1 | INTRODUCTION

Adaptive metabolic evolution is a powerful technique for developing unique microbial biocatalysts for production of metabolites of economic interest.[1–3] This approach involves redirection of existing metabolic pathways by altering the regulation of gene expression, changing the biochemical properties of specific enzymes in the pathway to achieve the needed catalytic capacity and metabolic integration of newly acquired enzyme activity into host physiology. This technique harnesses the potential of the multitude of native genes with unknown function towards development of microbial biocatalysts for industrial applications.[3–5]

We previously developed a *Bacillus coagulans* strain that produced D-lactic acid.[6] This isolate was obtained after metabolic evolution of a *B. coagulans* strain engineered to be phenotypically anaerobic growth negative via disruption of its native fermentation pathways. Using adaptive metabolic evolution, an anaerobic growth plus mutant strain QZ19 was isolated that produced D-lactic acid by an alternate route. Acquired mutations which allowed reduction of pyruvic acid to D-lactic acid resided within the gene encoding glycerol dehydrogenase

(GDH having glycerol oxidation activity, UniProt Accession: A0A150JSL8, *Bc*GDH). A F245S change alone and together with a subsequent D121N change, both within the *Bc*GDH active site, allowed for lactate dehydrogenase activity (LDH having pyruvate reduction activity) in strain QZ19. Since none of the present day GDHs catalyze the reduction of pyruvate to lactate, the altered *Bc*GDH forms with a single F245S and double D121N/F245S changes represent novel LDH enzymes.

In this study, we compared the kinetic properties of native, F245S, D121N, and D121N/F245S forms of *Bc*GDH in the oxidation of a variety of short chain aliphatic diols and reduction of α-ketoacids. In addition, a X-ray crystallographic structure of *Bc*GDH-D121N/F245S from strain QZ19 was used to guide structure comparisons of ligand and cofactor bound GDH homologs. Our findings show that the F245S change is responsible for the occurrence of pyruvate reduction activity. Based upon protein structure comparisons the molecular interactions in the altered active-site that support efficient α-keto acid reduction are proposed.

Broader Audience Statement

A glycerol dehydrogenase that catalyzes the transformation of glycerol to dihydroxyacetone was altered through directed evolution efforts and resulted in the acquisition of a primary lactate dehydrogenase function. In this study the native glycerol dehydrogenase as well as three altered forms were biochemically characterized and a X-ray crystallographic structure model was obtained. Findings indicate that opening of the substrate binding region and related changes to the hydrogen bonding network support the preferential binding of pyruvate by the altered enzyme.

2 | RESULTS

2.1 | Biophysical properties of *Bc*GDH native and altered forms

The native *B. coagulans* GDH had an apparent molecular mass of 86,000 Da as determined by size exclusion chromatography, a value that is consistent with a dimeric quaternary structure (39,000 Da per monomer). Activity of the protein increased by 1.9 fold following dialysis against $ZnCl_2$ supporting the previously demonstrated presence of a catalytic Zn^{2+} in the close homolog from *Geobacillus stearothermophilus*.[7] From this finding, the *Bc*GDH produced in *Escherichia coli* is suspected to be at least partially depleted of Zn^{2+}, an observation not uncommon in protein expression of metal dependent enzymes when trace metals are not included in the expression culture. The pH optimum for the native *Bc*GDH glycerol oxidation was approximately 9.0 (Figure 1a) and the temperature optimum was between 65 and 75 C (Figure 2a, inset), a value that is slightly higher than the optimum growth temperature of 55 C for the bacterium.[8] These biophysical aspects of *Bc*GDH are similar to those determined previously for GDH enzyme homologs.[7,9,10] The reduction of pyruvate by the altered forms of *Bc*GDH was shown to yield exclusively D-lactic acid using chiral HPLC. The pH and temperature optima of the *Bc*GDH-F245S enzyme form for glycerol oxidation were comparable to that of the native enzyme (Figures 1b and 2a) while the pH optimum for *Bc*GDH-F245S pyruvate reduction activity was 5.0 (Figure 1b) and at this pH, the enzyme was maximally active over a broad temperature range spanning 40–65 C (Figure 2b). For the *Bc*GDH-D121N/F245S form, the optimum GDH reaction temperature was observed at 60 C (Figure 2a). For pyruvate reduction activity, this GDH form also showed a broad maximum temperature range similar to that observed for the F245S GDH form (Figure 2b).

Thermostability studies indicated that at the optimum reaction temperature of 70 C, *Bc*GDH was inactivated, losing about 95% of its activity in less than 1 hr. In contrast, *Bc*GDH-F245S lost 30% of its glycerol oxidation activity during the first 15 min of incubation at 70 C yet retained approximately 60% of its activity even after 8 hr of incubation at 70 C, indicating a slightly higher temperature stability for this GDH form. The native enzyme was stable at 4 C for over 50 days while greater than 80% of the activity was lost when stored in 20% (vol/vol) glycerol or 15% (vol/vol) DMSO at −75 C (data not shown).

2.2 | Consideration of pyruvate reduction assays

Given pyruvate's absorption spectra which overlaps with the 340 nm absorption wavelength commonly utilized for NAD(H) studies and the high K_m for this substrate by the *Bc*GDH enzyme forms, the pyruvate reduction assay required special consideration. To accommodate this, NADH absorption data acquisition was shifted to 360 nm, the NADH concentration was used at only 2–3 times its K_m and the earliest rate data was utilized for calculations. While the K_m and V_{max} of the described optimal pyruvate reduction approach is provided in Table 2,

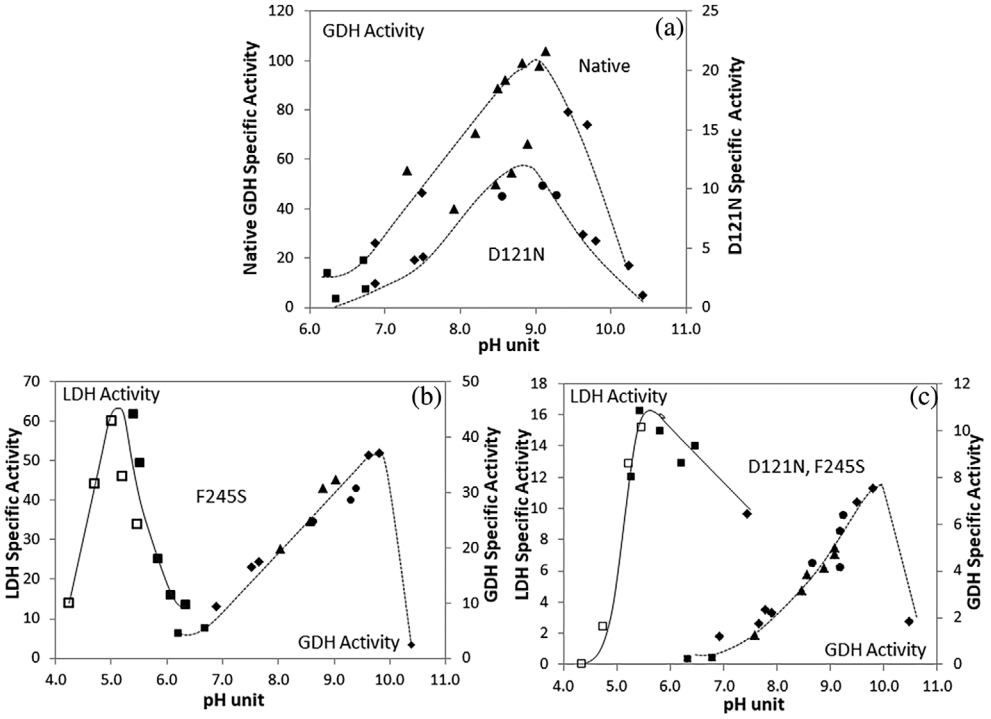

FIGURE 1 pH profiles of *Bc*GDH and its mutationally altered derivatives. Glycerol oxidation activity of the native and D121N form are shown in (a), for the F245S GDH form, both GDH and LDH pH optimums are shown in (b) and for the D121N/F245S two amino acid change both GDH and LDH activities are depicted in (c). Glycerol or pyruvate (100 mM) was present as the substrate in a reaction mixture that was buffered with MES (filled squares), phosphate (filled diamonds), CAPSO (filled triangles), carbonate (filled circles) or succinate (open squares) at 125 mM. Enzyme reaction was carried out at 60 C in a circulating water jacketed cuvette holder

the k_{cat} and specificity constant (k_{cat}/K_m) for pyruvate reduction were calculated using the V_{max} obtained from the NADH cofactor kinetic analysis. We thought this approach superior in consideration of the compromise required for the pyruvate reduction assay.

2.3 | Functional specificity of native *Bc*GDH

In addition to glycerol, the native *Bc*GDH also catalyzed oxidation of various diols (Table 1). Notably, several of the tested 1,2-diols showed specific activity comparable to that of glycerol. With ethanediol and D-2,3-butanediol, the specific activity was approximately 40–50% of the native glycerol oxidation activity. Additionally, 1,3-butanediol was not a good substrate for the enzyme and the activity with 1,4-butanediol was only marginally detectable. No activity was determined with 2, 3 or 4-carbon alcohols having alcohol substituents on a terminal carbon. These results suggest that *Bc*GDH has broad substrate specificity but a strict requirement for vicinal hydroxyls as substrate for the oxidation reaction with a preference for D-isomers of the tested diols.

2.4 | Kinetic evaluation of native *Bc*GDH

The affinity of native *Bc*GDH for glycerol was lower than that of D-1,2-propanediol (apparent K_m values of 4.0 and 1.0 mM, respectively) (Table 2) providing a rationale for the increased activity observed for D-1,2-propanediol. The observed difference in the specific activity of the enzyme on 1,2-butanediol and D-2,3-butanediol can also be correlated with the apparent K_m for these alternative substrates (Tables 2 and 3). Other kinetic properties of the enzyme with these substrates are comparable and based on the k_{cat}/K_m (Table 3), the preferred substrate appears to be D-1,2-propanediol. These results are in agreement with GDH enzymes isolated from *G. stearothermophilus* and *E. coli* that are capable of oxidizing 1,2-ethanediol, 1,2-propanediol and 2,3-butanediol.[7,9]

Native *Bc*GDH reduced pyruvate at 2.3 U mg^{-1} (Table 1). In these assays, the NADH concentration used was 3-times the apparent K_m for NADH and should not be significantly rate-limiting. Based on the calculated V_{max} values, the pyruvate reduction activity of the native *Bc*GDH was about 5% of the glycerol oxidation activity (Table 2). The low pyruvate reduction activity of this enzyme could be attributed to the very high apparent K_m for pyruvate (0.2 M; about 50-times higher than the value

for glycerol) (Table 2), indicating that the native *Bc*GDH has a very low affinity for pyruvate. Overall, the specificity constants (k_{cat}/K_m) indicate that the native enzyme is nearly 600-times more efficient oxidizing glycerol than it is at reducing pyruvate. *Bc*GDH also reduced 2-ketobutyric acid, but at only a 7.5-fold lower rate of

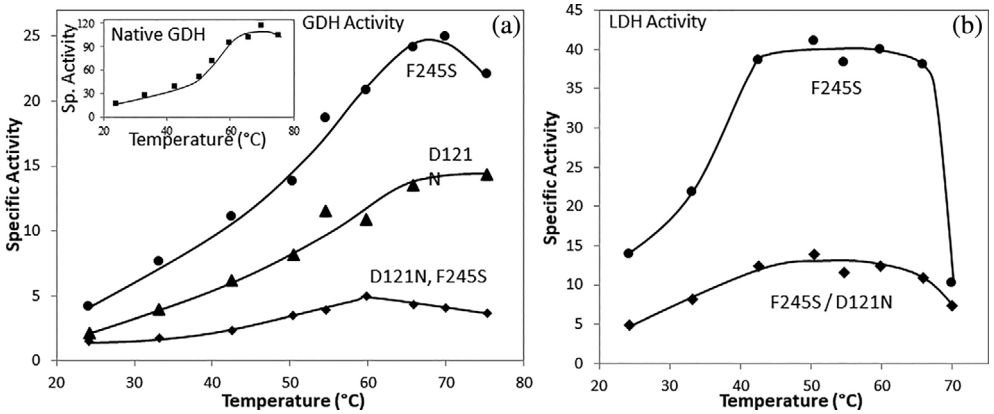

FIGURE 2 Temperature profile of *Bc*GDH and its mutationally altered derivatives. GDH reaction temperature optimum for all four enzyme forms are shown in (a) and for the F245S and D121N/F245S amino acid changes LDH temperature optimum is shown in (b). Enzyme reactions were carried out at the optimum pH value for each reaction (pH 8.9 for GDH and pH 5.4 for LDH) with glycerol or pyruvate at 100 mM. NAD^+ reduction or NADH oxidation was monitored at the indicated temperatures in a water-jacketed cuvette holder

TABLE 1 GDH and LDH activities of native *Bc*GDH and its altered forms

Substrate	Native	F245S	D121N	D121N/F245S
Glycerol	68.8	17.1	11.6	4.0
1,2-ethanediol	34.2	0.3	9.7	0.2
D,L-1,2-propanediol	72.0	47.2	15.4	23.9
D-1,2-propanediol	63.3	67.3	19.5	30.4
L-1,2-propanediol	14.1	3.2	2.2	1.0
1,2-butanediol	73.4	45.5	41.8	20.3
1,3-butanediol	8.0	1.8	1.6	0.2
1,4-butanediol	0.1	0.1	0.03	UD
D-2,3-butanediol	27.6	66.8	5.9	31.2
L-2,3-butanediol	0.2	1.0	0.4	0.5
Ethanol	0.2	0.3	2.7	0.2
Isopropanol	UD	UD	0.8	0.5
1-butanol	0.1	0.04	0.3	0.04
2-butanol	0.02	0.05	0.04	0.03
Pyruvate	2.3	38.3	0.1	11.7
2-ketobutyric acid	0.3	29.8	UD	6.1
D,L-lactate	UD	0.3	0.1	0.8
D-lactate	UD	0.3	UD	1.0
L-lactate	UD	0.1	UD	0.01
D,L-malate	0.1	UD	0.1	UD

Note: Enzyme activities were determined at 55 C at a substrate concentration of 100 mM. Specific activity is expressed as μmoles min^{-1} mg $protein^{-1}$. L-2,3-butanediol was dissolved in 2-butanol and the concentration of 2-butanol in the assay was 4%. Addition of 2-butanol at 4% to a reaction with glycerol as substrate had no significant effect on the activity of the enzyme. LDH forward reaction followed the reduction of pyruvate (or 2-ketobutyric acid) with NADH and the reverse reaction was followed by the oxidation of lactate (or malate) as substrate. See Methods section for other details. UD, undetectable; less than 0.01 unit of enzyme activity.

pyruvate and had no activity with oxaloacetate as substrate (Table 1).

2.5 | Kinetic evaluation of *Bc*GDH F245S

For the *Bc*GDH-F245S form, the rate of glycerol oxidation decreased by about 75% and the pyruvate reduction activity increased about 17-fold (Table 1). The difference in the GDH and LDH activities for *Bc*GDH-F245S could be attributed to an increase in apparent K_m for glycerol (41.0 mM vs 4.0 mM for the native enzyme) and a reduction in apparent K_m for pyruvate (54.5 mM vs. 207 mM for the native enzyme) (Table 2). The substrate specificity constant for *Bc*GDH-F245S with pyruvate as substrate increased to 6.5 compared to 0.05 mM^{-1} s^{-1} for the native enzyme (Table 3). While this enzyme form gained significant pyruvate reduction activity, the catalytic efficiency of this reaction was only about 20% of that measured for the glycerol oxidation by the native *Bc*GDH. The *Bc*GDH-F245S enzyme also had very low, but detectable, lactate oxidation activity indicating that the reverse reaction does not occur efficiently (Table 1).

Although the F245S form of *Bc*GDH had a significantly lower oxidation activity with glycerol and other substrates, the D-1,2-propanediol oxidation activity was not significantly changed compared to the native enzyme (Table 1). The increased affinity for D-2,3-butanediol was also accompanied by an improved k_{cat} with this substrate (Tables 2 and 3).

2.6 | Kinetic evaluation of *Bc*GDH-D121N

In the directed evolution studies, the D121N GDH form was not identified as a singular change, since it appeared only following the F245S alteration.[6] However, in this

TABLE 2 Kinetic properties of *Bc*GDH and its altered forms with LDH activity

Substrate	Apparent K_m (mM)				V_{max} [a]			
	Native	F245S	D121N	D121N/F245S	Native	F245S	D121N	D121N/F245S
Glycerol	4.0	41.0	195.0	148.0	82.0	30.0	35.0	7.5
D-1,2-propanediol	1.0	4.5	19.0	8.0	64.0	61.0	20.0	30.0
1,2-butanediol	3.0	23.5	4.0	44.0	84.0	50.0	46.5	34.0
D-2,3-butanediol	17.0	6.5	90.0	39.0	36.0	95.0	7.5	40.0
NAD^+	0.4	0.7	1.5	2.3	78.0	25.0	35.0	ND
Pyruvate	207.0	54.5	60.5	55.5	3.8	61.7	0.2	14.4
NADH	0.05	0.1	0.1	0.3	7.0	245.0	1.0	115.0
LDH/GDH					0.05	2.06	0.01	1.92

Note: Concentration of NAD^+ or NADH in the reaction mixture was 3.3 mM or 0.125 mM, respectively. The V_{max} values obtained with varying NAD^+ concentration was determined with glycerol (0.1 M) as the substrate. As detailed in the Results section, the pyruvate reduction kinetic values are taken in consideration of the reaction limitations resulting from overlapping absorption of pyruvate and NADH and the high K_m for pyruvate. The reaction temperature was 55 C.

[a]μmoles min^{-1} mg $protein^{-1}$.

TABLE 3 k_{cat} and k_{cat}/K_m of *Bc*GDH and its altered forms with LDH activity on various substrates

Substrate	k_{cat} (s^{-1})				k_{cat}/K_m (mM^{-1} s^{-1})			
	Native	F245S	D121N	D121N/F245S	Native	F245S	D121N	D121N/F245S
Glycerol	117.5	42.5	50.0	11.0	30.0	1.0	0.3	0.1
D-1,2-propanediol	92.0	87.5	29.0	42.5	92.0	20.0	1.5	5.5
1,2-butanediol	120.5	71.0	66.5	50.0	40.0	3.0	15.5	1.0
D-2,3-butanediol	50.5	136.0	10.5	57.5	3.0	21.0	0.1	1.5
Pyruvate[a]	10.5	352.0	1.5	165.0	0.05	6.5	0.02	3.0

[a]Since the concentration of NADH and pyruvate in the pyruvate reduction assay is not ideal for kinetic determination (see results section), k_{cat} was calculated from the V_{max} values obtained with varying NADH concentration, listed in Table 2.

study, we sought to identify its separate contribution to pyruvate reduction activity. The D121N change lowered the activity of the enzyme with most all the tested substrates relative to the native enzyme (Table 1). Interestingly, while the rate of glycerol oxidation decreased by approximately seven-fold to 11.6 U mg^{-1} the rate of pyruvate reduction activity fell from the already low 2.3 U mg^{-1} for the native *Bc*GDH to 0.1 U mg^{-1} for the D121N form. In consideration of the specific activity (Table 1), this singular change has no beneficial effect on either GDH or LDH activities. The only exception to this is the measured oxidation of ethanol which increased to 2.7 U mg^{-1} from the 0.2 U mg^{-1} determined for the native *Bc*GDH. The lower activity of the *Bc*GDH-D121N can be correlated to the lower affinity of this enzyme to these substrates (Table 2). These results suggest that Asp121 is important for both the GDH and LDH activities of the enzyme. It is possible that the mutation leading to D121N change was selected during metabolic evolution to modulate the enzyme activity of the F245S form for physiological reasons.

2.7 | Kinetic evaluation of *Bc*GDH-D121N/F245S enzyme form

Combining the *Bc*GDH-D121N change with the F245S change partially restored the activities of the enzyme with many substrates (Table 1). While all specific activities are decreased relative to the single F245S alteration, the measured values are not an order of magnitude lower and, in many cases, are significantly higher than the D121N GDH. The GDH and LDH activities decreased fourfold and threefold, as compared to the single F245S form, respectively. The still significant LDH activity of 11.7 U mg^{-1} measured for the D121N/F245S enzyme form contrasts with the very low LDH activity for the D121N change alone. The D121N/F245S form showed the highest lactate oxidation reaction rate of 1 U mg^{-1}. The k_{cat} for the *Bc*GDH-D121N/F245S with pyruvate as substrate is about 16-fold higher than that of the native enzyme (Table 3).

2.8 | Apo-*Bc*GDH structure determination

The D121N/F245S form of *Bc*GDH crystalized in the C2221 space group and diffracted to 2.4 Å (Table 4). The unit cell was relatively large and solvent content was determined to be 54.2%. Overall, the data was 96.1% complete and 3.3-fold redundant. The unit cell contained 8 chains of *Bc*GDH being composed of 2 tetrameric rings (Figure 3a). An octameric quaternary structure has also been proposed for the *Gs*GDH enzyme.[10] The *Bc*GDH form that crystallized contained no cofactors or substrate. Although no additional zinc was added to the *Bc*GDH prior to crystallization efforts it was surprising to find that the protein structure contained no density for a coordinated Zn^{2+} and the Zn^{2+} coordinating side chains showed low quality density and increased B-factors. The primary factor affecting *Bc*GDH coordination of Zn^{2+} is considered to be the high levels of citrate in the crystallization condition which would effectively chelate the catalytic Zn^{2+}.[11,12]

In this structure, the two altered amino acids, D245S and D121N, reveal the conformation of these alternative amino acid side chains. In the *Gs*GDH NAD^+/Zn^{2+} bound structure D123 (D121 equivalent in *Bc*GDH) hydrogen bonds with a water which is involved in Zn^{2+} coordination prior to substrate recruitment (Figure 3b). As modeled in the apo-*Bc*GDH D121N/F245S structure, the $O^{\delta1}$ of N121, is oriented up and would then be expected to maintain the integrity of the water Zn^{2+} ligand interaction. However, the $N^{\delta2}$ is oriented downward and the addition of these two amino hydrogens likely perturbs the hydrogen bonding network of the substrate binding pocket (Figure 3c).

As can be seen from the F245S form of the apo-*Bc*GDH enzyme the substrate binding pocket

TABLE 4 Data collection and processing

Diffraction source	Beamline 22-ID, APS
Wavelength (Å)	0.9794
Temperature (K)	100
Detector	ADSC Quantum 315r CCD
Space group	*C*2221
a, *b*, *c* (Å)	211.67, 211.77, 149.43
α, *β*, *γ* ( )	90.00, 90.00, 90.00
Solvent content (%)	54.2
Resolution range (Å)	49.9–2.40 (2.44–2.40)[a]
Total no. of reflections	798,856
No. of unique reflections	126,259 (11,943)
Completeness (%)	96.1 (89.5)
Redundancy	3.3 (3.3)
$\langle I/\sigma(I)\rangle$	17.3 (2.3)
$CC_{1/2}$	0.904
$R_{p.i.m.}$	0.057 (0.210)
Overall *B* factor from Wilson plot ($Å^2$)	27.1

[a]Values in parentheses are for the highest resolution shell (2.44–2.40 Å).

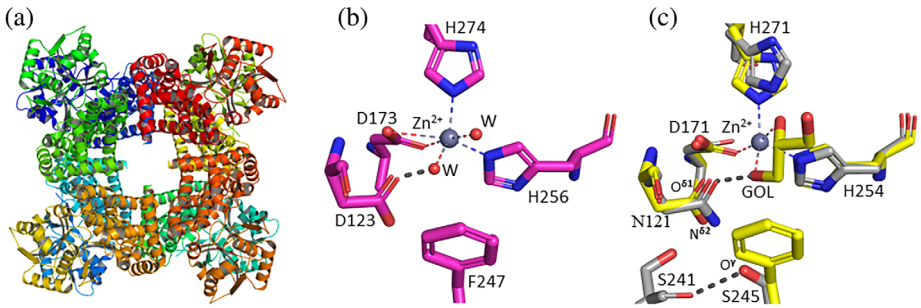

FIGURE 3 Comparative protein structure characteristics of apo-*Bc*GDH-D121N/F245S *Bc*GDH. The unit cell contained eight *Bc*GDH chains arranged into two stacked tetramers (a). Zn^{2+} substrate binding site of the *Gs*GDH (PDB code: 1JPU, magenta, amino acid numbering according to *Gs*GDH) showing the amino acids and waters involved in Zn^{2+} coordination as an example of a wild-type structure model (b). Apo-*Bc*GDH-D121N/F245S enzyme form aligned with glycerol (GOL) and the Zn^{2+} bound form of *Gs*GDH (PDB code: 1JQA, yellow, amino acid numbering according to *Bc*GDH) (c)

substantially opens by replacing the large hydrophobic phenylalanine with the much smaller polar serine. The structure also reveals that whereas F245 is oriented directly vertical in the pocket the S245 angles toward N121 and establishes a strong hydrogen bond as a hydrogen donor to the main chain carbonyl oxygen of S241 (Figure 3c). This interaction, or an equivalent is not possible in the wild-type F245 form of the enzyme. Further, the O^{γ} of S245 is additionally available in the substrate binding pocket for further hydrogen bond interactions as a hydrogen acceptor. This also disrupts the hydrogen bonding network of the evolved GDH function. Although close, it is not expected that the N121 and S245 establish a hydrogen bond due to unfavorable geometry.

2.9 | Structural evaluation of the alternative GDH forms

Explanations for the kinetic results were developed from structural comparisons of the *Bc*GDH-D121N/F245S X-ray crystallographic structure model (PDB code: 6CSJ; this work) with the NAD^+ and glycerol bound structures of *Gs*GDH (PDB codes: 1JQ5 and 1JQA, respectively) and provides insight into the differences between glycerol and pyruvate coordination. From the earlier ligand and cofactor bound *Gs*GDH structures, a network of hydrogen bonding interactions was proposed which identified an important role for the hydroxyl groups of glycerol closest to the catalytic Zn^{2+} ion (Figure 4a).[10] In this current report, our analysis is based on the hypothesis that pyruvate is positioned within the active site in proximity to the catalytic Zn^{2+} ion and NAD(H) cofactors in a manner analogous to that observed for glycerol in the native enzyme (Figure 4b). This is the most likely scenario for the reduction of pyruvate since neither of the two amino acid changes are predicted to disrupt the positioning of the Zn^{2+} catalytic center nor NAD(H) binding. As such, it is highly likely that these enzymatic cofactors interact with pyruvate in the *Bc*GDH-D121N/F245S enzyme form for reduction of the C-2 carbon of pyruvate in a manner analogous to that observed in the glycerol bound *Gs*GDH crystallographic model.

In the binding of glycerol by the native *Bc*GDH, the C-1 and C-2 hydroxyl oxygens of glycerol are involved in coordinate bonds with Zn^{2+}, while the hydrogen atoms of those hydroxyl groups are involved in hydrogen bonding interactions. If pyruvate was bound by the native *Bc*GDH, similar hydrogen bonding would not occur because the more oxidized pyruvate only contains a single hydrogen which can be donated in a manner similar to glycerol (Figure 4c). We hypothesize that changes to *Bc*GDH that increase pyruvate reduction activity likely function by providing an increase in hydrogen bonds for the more oxidized substrate pyruvate, thereby allowing the molecule to be stably bound and reduced.

From the *Gs*GDH crystallographic models Phe-247 (Phe-245 in *Bc*GDH) serves as a "wall" in the active site, setting the limits of glycerol C1 penetration into the substrate pocket and helping to position C2 and its hydroxyl substituent near the Zn^{2+} and NAD^+ ring for oxidation (Figure 4a). The change of this phenylalanine to the smaller, polar serine (F245S form of *Bc*GDH) increases the volume of the substrate binding site while simultaneously altering it from having a back-side hydrophobic surface to a polar one capable of acting as both a hydrogen bond donor and acceptor. Such changes would be expected to favor binding of substrates with greater polar character at C1 such as pyruvate (Figure 4b,c), a hypothesis that is supported by the data obtained for the BcGDH-F245S enzyme form.

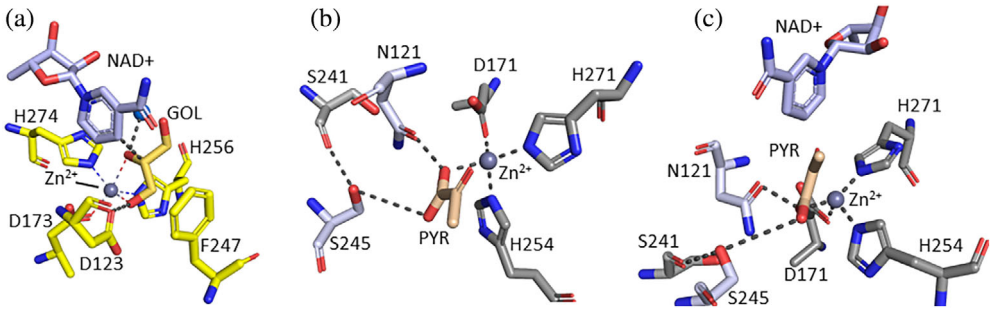

FIGURE 4 Modeling of pyruvate (PYR) into the *Bc*GDH-D121N/F245S structure model. *Gs*GDH ternary complex assembled from alignments of two *Gs*GDH structures (PDB codes: 1JQA and 1JQ5) showing all contacts which are thought to occur during the oxidation of glycerol to dihydroxyacetone, including a line connecting the C2 of glycerol to the C4N carbon of NAD^+ indicating the trajectory of the hydride transfer (a). *Bc*GDH-D121N/F245S structure model derived from an alignment with *Gs*GDH models (PDB codes: 1JQA and 1JQ5) containing pyruvate in the active site as described in the Results section. For this figure, the position of NAD^+ (not shown for clarity in 4b), Zn^{2+} and the three Zn^{2+} coordinating amino acid side chains are taken from the *Gs*GDH structure (PDB code: 1JQA) and shown in darker grey. *Bc*GDH amino acid positions are shown in lighter grey (b). In (c), an alternative perspective is provided of (b) showing potential hydrogen bonds which help to explain lactate dehydrogenase activity. Specifically, the possibility of the hydrogen bonding of the O1 of pyruvate with the S245 hydroxyl is indicated

3 | DISCUSSION

One explanation for the significantly decreased glycerol oxidation activity of the *Bc*GDH-D121N form is that the local hydrogen bonding network is perturbed possibly disrupting glycerol recruitment. The negative impact of the D121N change on pyruvate reduction activity is largely alleviated when the F245S alteration is included indicating that opening the pocket and providing a polar interaction point counteracts the D121N single change detriment.

The combination of the two active site alterations and the change in the oxidation state of the substrate (glycerol to pyruvate) has essentially swapped the role of hydrogen bond donor from the substrate (glycerol hydroxyl moieties) to the enzyme (serine hydroxyl and asparagine amide groups) and that of hydrogen bond acceptor from the enzyme (aspartate carboxylate) to substrate (pyruvate carboxylate). When combined with the added space resulting from the removal of the phenyl group of phenylalanine, the result is an active site pocket that is capable of stably binding pyruvate (Figure 4b) and positioning it for subsequent reduction.

In the case of F245S *Bc*GDH form alone, it is interesting to find a single mutation that converts an enzyme with GDH activity to one with D-LDH activity given that there is no apparent similarity between the GDH and LDH enzyme families other than their inclusion of significantly different forms of the Rossman fold for dinucleotide (NAD(H)) binding.[10]

Efforts in rational design or protein library screening of enzymes which seek to obtain new substrate specificities are costly, difficult and often met with limited success. Another major drawback of these alternative approaches is that a suitable protein needs to be identified as an engineering template. However, in the application of adaptive metabolic evolution of an organism, as in this case, the selective pressure is applied across the breadth of the entire microbial proteome, thereby boosting the likelihood of success. In addition, metabolic evolution is also expected to select a combination of beneficial changes that support optimal growth of the microorganism in that environment, although an individual mutation by itself may not be effective. In this case, with the *Bc*GDH, the process resulted in the mutation of the DNA of a functionally similar, but non-homologous enzyme; with the new resulting enzyme gaining D-LDH activity that allowed for enhanced growth of *B. coagulans* strain QZ15.[6] The result is not surprising given the similarity between target substrates and the inherent dehydrogenase function shared by these two enzymes. It seems possible that the GDH enzyme may be apt by its very nature to be amenable to active site alterations. Notably, these enzymes, sometimes referred to as diol dehydrogenases due to their ability to oxidize diols other than glycerol, have broad substrate specificity. In the same vein, one wonders if a native lactate dehydrogenase might successfully be converted to a glycerol dehydrogenase given an appropriate selective pressure. Inspection of the structures of these enzymes and a review of the literature identifies a mobile loop which closes in upon pyruvate binding and facilitates reduction of the C-2 ketone by stabilizing the oxoanionic transition state via an interaction with arginine.[13] In such an intricate case, active site changes may not so easily be accommodated.

The higher activity of the F245S enzyme with various short chain diols coupled with its thermophilic characteristics (optimum of 70 C) makes this enzyme useful in bioconversion of various diols and polyols to corresponding ketones with stereoselectivity as potential pharmaceutical intermediates of commercial interest.

4 | MATERIALS AND METHODS

4.1 | Materials

Biochemicals were from Sigma Chemical Co. (St. Louis, MO). Analytical grade organic and inorganic chemicals were from Fisher Scientific (Pittsburgh, PA). Molecular biology reagents and supplies were from New England Biolabs (Ipswich, MA), Invitrogen (Carlsbad, CA) or Bio-Rad Laboratories (Hercules, CA). PCR primers were synthesized by Invitrogen. Chromatography column materials were from GE Healthcare (Marlborough, MA).

4.2 | Construction of expression plasmids and protein expression

The *Bc*GDH-D121N/F245S expression vector, pQZ113, was constructed previously[6] by cloning the *Bc*GDH gene from the genomic DNA of *B. coagulans* strain QZ19 into the XhoI/BamHI linearized pET15b expression vector (Novagen, Inc.) with the N-terminal Hexa-Histidine tag for affinity purification. Using the same primers and genomic DNA from the wild-type *B. coagulans* strain P4-102B the DNA encoding the native form of *Bc*GDH was cloned for expression as above to make pQZ117.[6] Construction of expression plasmids with the *Bc*GDH-F245S (pQZ118) and *Bc*GDH-D121N (pQZ119) utilized inverse PCR using pQZ113 as template and non-overlapping primers, one of which carrying the required mutation. The entire approximately 7 kb DNA was amplified, self-ligated following phosphorylation and transformed into *Escherichia coli* DH5α for propagation. Purified expression plasmids were transformed into *E. coli* strain Rosetta (DE3) (Novagen, Inc.) for high level production of respective proteins.

4.3 | Protein expression and purification

For expression of native and the three variants of *Bc*GDH-(D121N; F245S; D121N/F245S), 350-ml LB + ampicillin cultures (in 2.8-l Fernbach flasks) were grown at 37 C with shaking at 200 RPM to an optical density at 420 nm of about 0.8 (Beckman DU640 spectrophotometer). Isopropyl β-D-1-thiogalactopyrano side was added at 50 μM for protein induction and the rotation speed was increased to 250 rpm. After 4 hours at room temperature, cells were harvested by centrifugation (10,000 × *g*, 10 min, 4 C), washed with 25 ml of 50 mM potassium phosphate buffer, pH 8.0 and the cell pellet was suspended in 3 ml of the same buffer but containing EDTA-free protease inhibitors (Fisher Scientific). Cells were passed through a pre-chilled French pressure cell at 20,000 PSI and the extract was collected on ice. All subsequent operations were conducted at 4 C. The crude extract was clarified by centrifugation (30,000 × *g*, 25 min), and the supernatant was filtered through a 0.22-μm filter. The cell free extract was passed through a HiTrap chelating column in the Ni^{2+} form (1 ml; GE Healthcare) equilibrated in 50 mM potassium phosphate buffer, pH 8.0 (BB). Unabsorbed and loosely bound proteins were removed from the column by washing with 5 column volumes of BB, followed by 5 column volumes of BB containing 50 mM imidazole. Amino-terminal hexahistidine-tagged GDH proteins were eluted with a linear gradient of 50 mM to 0.5 M imidazole in BB at a flow rate of 0.5 ml min^{-1}. All the fractions containing GDH activity were combined. The GDH proteins were further purified with a Sephacryl S-200 HR column (2.6 by 60 cm; GE Healthcare) equilibrated with BB containing 0.1 M NaCl at a flow rate of 0.5 ml min^{-1}. All fractions containing GDH activity were combined and dialyzed overnight against 125 mM HEPES at pH 8.0 containing 1 mM $ZnCl_2$. Using the same size-exclusion column, the native molecular weight of the proteins was determined with protein standards ovalbumin (45,000 Da), bovine serum albumin (66,000 Da) and alcohol dehydrogenase (150,000 Da). The purity and subunit mass of the protein was determined by sodium dodecyl sulfate-polyacrylamide gel electrophoresis (SDS-PAGE).[14] Protein concentration was determined by the Bradford assay using BSA as a standard.[15]

4.4 | *Bc*GDH pH and temperature optimization and temperature stability determination

A range of buffers was utilized to cover the full pH range. These include 2-(N-morpholino)ethanesulfonic acid (MES), phosphate 3-(Cyclohexylamino)-2-hydroxy-1-propanesulfonic acid (CAPSO), carbonate and succinate. These were used at 125 mM and pH optimization was performed at 60 C. For reaction temperature optimization, the optimum pH (pH 8.9 for GDH and pH 5.4 for LDH) was utilized over a temperature range of 25–75 C (max 70 C for LDH). For *Bc*GDH temperature stability

analysis, *Bc*GDH-F245S and *Bc*GDH-D121N were incubated at 70 C whereas *Bc*GDH-D121N/F145S was incubated at 60 C in 125 mM HEPES, pH 8.0. A sample of the protein was withdrawn at various times over an eight-hour period and the enzyme activity was determined at 55 C as described above. All reactions were initiated by addition of substrate, except as further detailed below.

4.5 | Enzyme assay and kinetic analysis

GDH activity was assayed by reduction of NAD^+ with glycerol as substrate based on a method reported previously with modification.[16] The reaction was carried out in a solution containing 125 mM CAPSO (Acros Organic), 60 mM $(NH_4)_2HPO_4$, pH 8.9, 3.3 mM NAD^+ and 0.5 to 4 μg of protein.

LDH activity was assayed by following the oxidation of NADH in the reduction of pyruvate. This was performed in 125 mM MES buffer at pH 5.4 with 60 mM $(NH_4)_2SO_4$, 0.125 mM NADH and 0.5 to 4 μg of enzyme, a modification of a previously reported method.[17] The identity of the lactate enantiomorph produced in this reaction was determined by HPLC (Agilent Technologies, Santa Clara, CA) using a Chirex 3,126 D-penicillamine column (Phenomenex, Torrance, CA) with 2 mM $CuSO_4$ as eluent.

Activities were measured using a Beckman DU640 spectrophotometer at 55 C. Reactions were initiated by the addition of 100 mM substrate following temperature equilibration and were followed at 360 nm instead of 340 nm to minimize interference by pyruvate. The extinction coefficient of NADH at 360 nm was determined as 4,334 M^{-1} cm^{-1}. One unit of activity was defined as the amount of enzyme that generates one μmole of product per minute. All substrates tested in this study were dissolved in water except L(+)-2,3-butanediol which was dissolved in 2-butanol. The final concentration of 2-butanol in the reaction mixture with 2,3-butanediol was 4% (v/v). GDH activity with glycerol as a substrate with this concentration of 2-butanol was comparable to the activity of control reactions without 2-butanol. The kinetic properties of each enzyme were determined as per Cornish-Bowden and the apparent K_m and V_{max} were calculated using Hanes plots.[18]

4.6 | X-ray crystallographic structure determination and structure analysis

Crystallization of *Bc*GDH-D121N/F245S was performed using the hanging drop method at room temperature. The drop contained 1 μl of *Bc*GDH-D121N/F245S in 50 mM potassium phosphate buffer, pH 8.0, 0.1 M NaCl, plus 1 μl of reservoir solution containing 0.2 M ammonium citrate, pH 4.5, 10% (wt/vol) PEG3350. Crystals grew within 48 hours and were allowed to grow for a minimum of 96 hours. Crystals to be used in data collection were cryoprotected in 30% glycerol, cryocooled at 100 K and mounted. Data were collected at Southeast Regional Collaborative Access Team (SER-CAT) 22-ID at the Advanced Photon Source, Argonne National Laboratory, Argonne, IL. Data were processed and integrated using HKL-3000.[19] The structure was solved by molecular replacement using MOLREP.[20] A single protein chain of the *Serratia* homolog (PDB code 4MCA; 58% sequence identity) was used as a search model. The model obtained after molecular replacement was rebuilt using Coot[21] and refined using REFMAC.[22] The near final structure was evaluated using the PDBRedo server.[23] After evaluation by PDBRedo, the model was further built and refined with REFMAC using the parameter file generated by the PDBRedo server. The final model, together with structure factors, was deposited in the Protein Data Bank[24] with accession code 6CSJ. Structure comparisons were performed using the X-ray crystallographic structure of *G. stearothermophilus* GDH (*Gs*GDH, PDB codes: 1JQA and 1JQ5).[10] Structure figures were prepared using PyMOL[25] (https://pymol.org/2/).

ACKNOWLEDGMENTS

This work was supported by funding from the U.S. Department of Energy's Office of Energy Efficiency and Renewable Energy, Bioenergy Technologies Office and sponsored by the U.S. Department of Energy's International Affairs award (DE-PI0000031) and by a grant from the US Department of Agriculture (2011-10006-30358). JCH is supported by a grant from the National Center for Research Resources (5 P20 RR016461). Use of the Advanced Photon Source was supported by the U. S. Department of Energy, Office of Science, Office of Basic Energy Sciences, under Contract No. W-31-109-Eng-38.

AUTHOR CONTRIBUTIONS

Diane Chauliac: Conceptualization; formal analysis; investigation; methodology; writing-original draft; writing-review and editing. **Qingzhao Wang:** Data curation; formal analysis; investigation; writing-review and editing. **Grace Jones:** Data curation; formal analysis; investigation. **Jason Hurlbert:** Conceptualization; formal analysis; investigation; resources; writing-review and editing. **Lonnie Ingram:** Funding acquisition; project administration; resources; supervision; writing-review and editing. **Keelnatham Shanmugam:** Formal

analysis; funding acquisition; project administration; supervision; writing-review and editing.

ORCID

Franz J. St. John https://orcid.org/0000-0003-3458-5628

REFERENCES

1. Cobb RE, Si T, Zhao H. Directed evolution: An evolving and enabling synthetic biology tool. Curr Opin Chem Biol. 2012;16:285–291.
2. Peralta-Yahya PP, Zhang F, del Cardayre SB, Keasling JD. Microbial engineering for the production of advanced biofuels. Nature. 2012;488:320–328.
3. Turner NJ. Directed evolution drives the next generation of biocatalysts. Nat Chem Biol. 2009;5:567–573.
4. el Hawrani AS, Sessions RB, Moreton KM, Holbrook JJ. Guided evolution of enzymes with new substrate specificities. J Mol Biol. 1996;264:97–110.
5. Jackel C, Hilvert D. Biocatalysts by evolution. Curr Opin Biotechnol. 2010;21:753–759.
6. Wang Q, Ingram LO, Shanmugam KT. Evolution of D-lactate dehydrogenase activity from glycerol dehydrogenase and its utility for D-lactate production from lignocellulose. Proc Natl Acad Sci U S A. 2011;108:18920–18925.
7. Spencer P, Bown KJ, Scawen MD, Atkinson T, Gore MG. Isolation and characterisation of the glycerol dehydrogenase from *Bacillus stearothermophilus*. Biochim Biophys Acta. 1989;994:270–279.
8. Patel MA, Ou MS, Harbrucker R, et al. Isolation and characterization of acid-tolerant, thermophilic bacteria for effective fermentation of biomass-derived sugars to lactic acid. Appl Environ Microbiol. 2006;72:3228–3235.
9. Tang CT, Ruch FE Jr, Lin CC. Purification and properties of a nicotinamide adenine dinucleotide-linked dehydrogenase that serves an *Escherichia coli* mutant for glycerol catabolism. J Bacteriol. 1979;140:182–187.
10. Ruzheinikov SN, Burke J, Sedelnikova S, et al. Glycerol dehydrogenase. Structure, specificity, and mechanism of a family III polyol dehydrogenase. Structure. 2001;9:789–802.
11. Glusker JP. Citrate conformation and chelation: Enzymic implications. Acc Chem Res. 1980;13:345–352.
12. Wyrzykowski D, Chmurzyński L. Thermodynamics of citrate complexation with Mn^{2+}, Co^{2+}, Ni^{2+} and Zn^{2+} ions. J Therm Anal Calorim. 2009;102:61–64.
13. Cameron JM, Levandovskiy V, Mackay N, et al. Novel mutations in dihydrolipoamide dehydrogenase deficiency in two cousins with borderline-normal PDH complex activity. Am J Med Genet A. 2006;140:1542–1552.
14. Laemmli UK. Cleavage of structural proteins during the assembly of the head of bacteriophage T4. Nature. 1970;227:680–685.
15. Bradford MM. A rapid and sensitive method for the quantitation of microgram quantities of protein utilizing the principle of protein-dye binding. Anal Biochem. 1976;72:248–254.
16. Lin EC, Magasanik B. The activation of glycerol dehydrogenase from *Aerobacter aerogenes* by monovalent cations. J Biol Chem. 1960;235:1820–1823.
17. Yoshida A, Freese E. Lactate dehydrogenase from *Bacillus subtilis*. Methods Enzymol. 1975;41:304–309.
18. Cornish-Bowden A. Fundamentals of enzyme kinetics. London: Portland Press, 1995.
19. Minor W, Otwinowski Z. Processing of X-ray diffraction data collected in oscillation mode. Methods Enzymol. 1997;276:307–326.
20. Vagin A, Teplyakov A. Molecular replacement with MOLREP. Acta Crystallogr. 2010;D66:22–25.
21. Emsley P, Cowtan K. Coot: Model-building tools for molecular graphics. Acta Crystallogr. 2004;D60:2126–2132.
22. Murshudov GN, Skubak P, Lebedev AA, et al. REFMAC5 for the refinement of macromolecular crystal structures. Acta Cryst D. 2011;67:355–367.
23. Joosten RP, Long F, Murshudov GN, Perrakis A. The PDB_REDO server for macromolecular structure model optimization. IUCrJ. 2014;1:213–220.
24. Berman HM, Westbrook J, Feng Z, et al. The protein data bank. Nucleic Acids Res. 2000;28:235–242.
25. DeLano WL. The PyMOL User's Manual. Palo Alto: DeLano Scientific, 2002.

How to cite this article: Chauliac D, Wang Q, St. John FJ, et al. Kinetic characterization and structure analysis of an altered polyol dehydrogenase with D-lactate dehydrogenase activity. *Protein Science*. 2020;1–11. https://doi.org/10.1002/pro.3963